Partial replacement of Portland-composite cement by fluidized bed combustion fly ash

Rissanen Jouni. [1], Ohenoja Katja. [2], Kinnunen Päivö. [3], & Illikainen Mirja. [4*]

[1] Doctoral student, Fibre and Particle Engineering, Faculty of Technology, PO Box 4300, 90014, University of Oulu, Finland

[2] D.Sc. (Tech.), Fibre and Particle Engineering, Faculty of Technology, PO Box 4300, 90014, University of Oulu, Finland

[3] Ph.D., Fibre and Particle Engineering, Faculty of Technology, PO Box 4300, 90014, University of Oulu, Finland

[4] Professor, Fibre and Particle Engineering, Faculty of Technology, PO Box 4300, 90014, University of Oulu, Finland

*Corresponding author

Abstract

Fly ash from fluidized bed combustion differs greatly from that of pulverized coal firing. The most noticeable differences are in morphology, reactivity, and chemical composition. The utilization of biomass fly ash from fluidized bed combustion as a cement replacement material could be a promising method for both minimizing the amount of landfilled fly ash and reducing CO_2 emissions in the concrete and cement industry. In this study, fly ash from fluidized bed combustion of peat and forest industry residue was used as a supplementary cementitious

material for CEM II composite cement which contains OPC, blast furnace slag, and limestone. Even with a 40% cement replacement ratio the compressive strengths of the mortar samples were still as high as 88% of the control sample's strength. Comparison with un-reactive replacement material revealed that moderate hydraulic properties of the studied fly ash explained the positive effects on strength rather than filler or nucleation effects.

Keywords: blast furnace slag, biomass ash, cement, hydration, mortar, reactivity

1. Introduction

Fluidized bed combustion is an efficient and growing method to produce energy from various fuel types such as coal, peat, wood, municipal waste, agricultural residues, etc. However, fluidized bed combustion produces significant amounts of fly ash, which can be hard to utilize. Annually 500 000 tons of fly ash originating from fluidized bed combustions of peat and wood is produced in Finland (Korpijärvi et al. 2009). More than 1.5 Mt/y similar ashes are produced in Europe (van Eijk et al. 2012) and, due to increasing demand for clean and renewable energy, the amount of fly ash is expected to increase in many regions. Utilization of fluidized bed combustion fly ash in concrete production as a cement replacement material could be a promising method to both minimize the amount of landfilled fly ash and to reduce CO_2 emissions created by the concrete and cement industry.

Fly ashes from fluidized bed combustion differ greatly from pulverized coal firing fly ash which has already been well studied (Abdul Awal 2013; Haha et al. 2010; Lawrence et al. 2005) and widely adopted by the concrete industry. The primary reasons for this are the differences in combustion conditions, fuel characteristics, and additive materials. The typical characteristics

of fluidized bed combustion fly ash are irregular, flaky particle size and a high portion of crystalline phases (Chindaprasirt et al. 2011; Li et al. 2012; Ohenoja et al. 2016b; Sinsiri et al. 2010; Zhao et al. 2015) which in generally are less reactive than amorphous phases. Pulverized coal firing produces spherically shaped fly ash (Li et al. 2012; Zhao et al. 2015), which has a high content of amorphous material (Chindaprasirt et al. 2011). Differences in physical ash characteristics are caused by different burning temperatures. In fluidized bed combustion, the temperature is kept low to reduce emissions and eliminate the sintering of ash particles (Loo et al. 2008). High temperatures in pulverized coal firing melt and sinter the ash particles and result in glassy spherical particles with more reactive phases (Chindaprasirt et al. 2011). Low temperatures lead to irregular particle shape (Zhao et al. 2015) with crystalline phases (Chindaprasirt et al. 2011).

In general, the chemical composition between the fly ashes from fluidized bed combustion varies more than fly ash from pulverized coal firing. Fluidized bed combustion is a suitable method for various fuels (e.g., coal, peat, wood, forest residues, agricultural residues, and municipal waste) and their combinations. Fuel mixtures and the quality of some fuels can vary significantly, even within a short period of time, which can cause fluctuations to ash quality. In addition to the fuel also possible fuel impurities, bed material and burning additives are present in the burning chamber. These materials can react in a boiler and alter the chemical composition of fly ash (Loo et al. 2008). One of the main advantages of fluidized bed combustion is that lime or dolomite can be injected into the boiler for the efficient reduction of SOx emissions, especially when coal is burned. Lime reacts with sulfur compounds, and sulfates are formed (Chindaprasirt et al. 2011; Zhao et al. 2015). The injection of lime or dolomite often explains the high CaO content of fly ash from the fluidized bed combustion of coal (Chindaprasirt et al. 2011; Zhao et al. 2015). Calcium containing compounds are not usually added to the combustion of biomass, but the calcium content of biomass fly ash can still be high because

some biomass fuels are so rich in calcium that it forms a significant portion of the fly ash. In some cases, calcium-containing sludge from the paper industry is injected into the boiler, which can increase the calcium content of the fly ash.

Utilization of fly ashes originating from fluidized bed combustion in cement applications has been investigated in several studies (Li et al. 2012; Nocuń-Wczelik et al. 2014; Pavoine et al. 2014; Rajamma et al. 2009, 2015; Roszczynialski and Nocuń-Wczelik 2004; Sinsiri et al. 2010; Wu et al. 2014; Zhao et al. 2015). Most of these studies are focused on fly ash from coal combustion and only few (Rajamma et al. 2009, 2015) on biomass fly ash. Similarly utilization of biomass fly ash has been studied (Berra et al. 2015; Cuenca et al. 2013; Kaminskas and Cesnauskas 2014; Kaminskas et al. 2015; Rajamma et al. 2015; Teixeira et al. 2016; Wang et al. 2008) but only on few cases (Rajamma et al. 2009, 2015) fluidized bed combustion is mentioned as a burning method. Additionally, in those studies where fly ash from fluidized bed combustion was used as a cement replacement material, clinker or Ordinary Portland Cement (CEM I or Type I) was used. However, some studies (Dung et al. 2014, 2015a; b; Salain et al. 2001; Wu et al. 2015) have suggested that fly ash from fluidized bed combustion could promote the hydration of blast furnace slag. Certain commercial cement types contain significant amounts of blast furnace slag; therefore, fly ash from fluidized bed combustion could more positively affect these cements. It should be noted that, due to variations in physical and chemical characteristics, the suitability of the ashes to work as a cement replacement material can vary significantly, and making conclusions based only on few studies should be avoided.

In this study, fly ash from fluidized bed combustion of peat and forest industry residues was used as a supplementary cementitious material for CEM II type cement which, in addition to clinker, contains blast furnace slag and limestone. Fly ash was milled to a fine particle size to enhance reactivity and ensure similar packaging with cement. As a reference, cement was replaced by un-reactive sand which was milled to the same particle size as cement. This method

has proven effective in identifying the different working mechanisms related to partial cement replacement (Lawrence et al. 2005; Sata et al. 2012). Investigations included the characterization of fly ash and milled sand, the analysis of the hydration heat by semi-adiabatic calorimetry, and evaluation of the properties of both fresh and hardened mortars.

2. Materials

The biomass fly ash used in this study originated from a 246 MW bubbling fluidized bed combustion boiler. During the gathering of ash samples, fuel composition was 80% peat and 20% forest industry residue. The temperature inside the boiler was approximately 890 °C which is typical for fluidized bed combustion. The fly ash used in this study was milled with a tumbling ball mill from original median particles size of 52.8 µm to approximately the same particle size as cement resulting in milled fly ash (MFA).

In this study, two different sands were used. Sand used as a cement replacement material was sieved natural sand (Puhallushiekka, Fescon) having an original particle size of 0.5–1.6 mm. This sand was composed of quartz, albite, and microcline. Before it was used as a cement replacement material, it was milled to the same particle size as cement with a tumbling ball mill resulting in milled sand (MS). Un-milled sand (UMS) was also used as a reference in the hydration heat studies.

The sand used as an aggregate material in the mortar was CEN-Standard sand (CEN-Standard, Normensand GmbH) which is described in cement testing standard EN 196-1 (SFS (Finnish Standards Association) 2016). The cement used in this study was type CEM II/B-M (S-LL) 42.5 N (Plussementti, Finnsementti). According to the manufacturer, in addition to clinker this cement contains 6–15% limestone and 15–25% blast furnace slag. A polycarboxylate-based superplasticizer agent (Sem®Flow ELE 20, Semtu) was used to adjust the consistency of mortar mixtures when 40% of the cement was replaced by biomass fly ash.

3. Methods

3.1. Chemical composition

An x-ray fluorescence method (XRF) was used to analyze the chemical compositions of fly ash, sand, and cement. The analysis was from melt-fused tablets using a wavelength dispersive XRF spectrometer (AxiosmAX, PANanalyctical). Loss on ignition of cement, MS, and fly ash at 950 °C were determined by heating the sample in the oven. Samples were kept in the oven overnight, and mass loss was calculated. Determination of the free CaO was done for fly ash using a method described in the fly ash testing standard EN 450-1 (SFS (Finnish Standards Association) 2013). Using this method, an ash sample was boiled for 3 h in a mixture of butanoic acid, 3-oxo-ethyl ester and butan-2-ol. Afterward, this mixture was filtered and titrated to determine the amount of free CaO. The selective dissolution method (Dyson et al. 2007; Haha et al. 2010; Luke and Glasser 1987) was used to evaluate the amount of reactive CaO, SiO_2, Al_2O_3, and Fe_2O_3. In this method, the ash sample was mixed in a solution consisting of ethylenediaminetetraacetic acid and triethanolamine solutions. The pH of the solution was adjusted to 11.6 ± 0.1, with the addition of 1 M NaOH. Concentrations of soluble CaO, SiO_2, Al_2O_3, and Fe_2O_3 were determined using the inductively coupled plasma technique.

3.2. Particle morphology

A field-emission scanning electron microscope (FESEM) (ULTRA PLUS, Zeiss) was used to analyze the particle morphology of both sand and fly ash. The samples were prepared by attaching the sample to a carbon sticker and sputter-coating it with platinum. The imaging of the samples was done using 5 kV voltage.

3.3. Particle size distribution

The analysis of particle size distribution of MFA, MS, and cement was done using a Beckman Coulter LS 13 320 laser diffraction particle size analyzer. Measurements were done using a dry powder system, and data was analyzed using the Fraunhofer optical model.

3.4. Preparation of mortar samples

The designs of the mortar mixtures are presented in Table 1. The control sample was prepared using cement, tap water, and CEN Standard sand. Milled sand was used to replace 10, 20, and 40% of the cement in the samples which are later referred to as MS 10%, MS 20%, and MS 40%, respectively. Similarly the samples in which cement were replaced with milled biomass fly ash are later referred to as MFA 10%, MFA 20%, and MFA 40%. Preparation of mortar samples was done according to cement standard EN 196-1 (SFS (Finnish Standards Association) 2016) with slight modifications. Modifications included the flow table test done before molding the samples and curing at a slightly higher temperature of 22.5 °C. Additionally, adjustments were made to mortar consistency using super plasticizer in the samples where 40% of the cement was replaced by MFA.

3.5. Heat of hydration

A semi-adiabatic calorimeter (F-Cal 8000, Calmetrix) was used to evaluate the heat of hydration of mixtures containing cement, water, and replacement materials. Samples were prepared using the same procedure as with the mortar samples with the exception that CEN Standard sand and plasticizer agent were not used. An equivalent amount of sand was used as a reference material in one sample container. The temperature of this reference was subtracted from the temperatures of other samples to determine the temperature change due to exothermic reactions and to eliminate possible external error sources.

3.6. X-ray diffraction analysis

A diffractometer (SmartLab, Rigaku) was used to identify crystalline phases of replacement materials and hardened cement pastes. The step interval, integration time, and angle interval used were 0.02 °, 0.24 s, and 10–90 °, respectively. Preparation of the hardened pastes included crushing, vacuum freeze drying, and grinding.

3.7. Consistency of fresh mortar

Consistencies of fresh mortar mixtures were evaluated using a flow table test described in mortar testing standard EN 1015-3 (SFS (Finnish Standards Association) 1999). The consistency was evaluated to ensure the proper rheology of the mortar mixtures and to estimate the water demands of both MFA and MS.

3.8. Strength measurements

Flexural strength was measured from 40*40*160 mm mortar prisms. Broken halves from the determination of flexural strength were used for compressive strength measurements. Both measurements were done according to cement testing standard EN 196-1 (SFS (Finnish Standards Association) 2016). Strength measurements were made after 2, 7, 28, and 90 d.

4. Results and discussion

4.1. Characterization of cement replacement materials

The chemical properties of the cement, MS, and fly ash are presented in Table 2. The fly ash was mainly composed of Si, Ca, Fe, and Al; however, it also contained alkalis, phosphates, sulfides, magnesia, and small quantities of Titanium and chloride. The selectively soluble portion of CaO was high, unlike with SiO_2, Al_2O_3, and Fe_2O_3. The fly ash contained some free CaO. The MS was mainly composed of silica and aluminum; however, it also contained some calcium, iron, sodium, and potassium. The low LOI value of the fly ash indicated that the amount of unburned carbon and carbonates were quite low. The higher LOI value of cement

likely resulted from the decomposition of carbonates present in the cement due to limestone which was one component of the cement used in this study.

The particle size distributions of cement, MS, and MFA are presented in Fig. 1 which shows that, after milling, the particle size distributions of cement, MS, and MFA were relatively wide and quite close to each other. After milling, MS and MFA still had a slightly higher fraction of particles exceeding 40 µm compared with cement; otherwise, the differences between materials were low. Thus, variations in particle size distributions of different materials should have a minimal effect on the packing of cement.

FESEM pictures of MFA and MS, which are presented in Fig. 2, revealed that the fly ash had an irregular morphology (Fig. 2b). In addition to irregularly shaped ash particles, few spherical particles were observed in the milled ash samples; however, their portion of all ash particles was low. The spherical shape of these particles originates from melting and sintering, which could suggest that these particles contain amorphous phases. MS possessed a more angular and solid particle shape than MFA (Fig. 2a). The BET surface areas of cement, MS, and MFA were 1.8, 2.2, and 2.7 m^2/g, respectively.

The XRD patterns of MS and MFA are presented in Fig. 3. XRD analysis of the MS revealed that the sand contained mainly quartz, albite, and microcline, which are all typical phases of Finnish sand. Fig. 3 shows that crystalline phases dominated the phase composition of MFA. Quartz, lime, anhydrite, albite, and hematite were identified from the XRD graph. The anhydrite content was estimated to be relatively low because the SO_3 content of the MFA was only 2.1%.

4.2. Heat of hydration

The results of the semi-adiabatic calorimetry are presented at Fig. 4. Figs. 4a and 4b present the heat of hydration for pastes when cement was replaced by MS and MFA, respectively. UMS was used as a reference, and the results are presented in Fig. 4c. When cement was replaced by

UMS the hydration heat dropped as the portion of sand increased. The occurrence of a heat peak was also slightly delayed (Fig. 4c). Regarding MFA, the hydration heat increased when 10% of the cement was replaced with MFA (Fig. 4b). A 10% cement replacement by MS produced a similar result when compared with the control sample (Fig. 4c). When a higher amount of cement was replaced by MS or MFA, the hydration heat decreased. Similar results are reported in literature: Fly ashes from pulverized coal firing (Abdul Awal 2013; Han et al. 2014) and from fluidized bed combustion (Nocuń-Wczelik et al. 2014; Rajamma et al. 2015) are known to decrease the hydration heat of cement.

At a replacement rate of 20%, the heat peaks of both MS and MFA were slightly higher than the heat peak of UMS sand; however, when 40% of the cement was replaced, the heat peaks of both MS and MFA were slightly lower than in UMS. This inconsistent result can be related to uncertainty of semi-adiabatic measurements. MFA raised the heat of hydration notably during the first 3 h (Fig. 4b) unlike UMS or MS. The effect was more pronounced as the replacement level increased. The early heat peak, which appeared in samples containing MFA (Fig. 4b), can be associated with the formation of ettringite (Han et al. 2014; Taylor 1997) and syngenite (Han et al. 2014). The ettringite has been found to be one of the main hydration products in self-hardening of these type of ashes (Illikainen et al. 2014). With MFA, the first peak clearly increased with the increasing replacement level. In addition to reactive Ca, the MFA contained reactive Al and Fe which are precursors of ettringite. Similar increase in early heat of hydration was also observed in a study by Nocuń-Wczelik et al. (Nocuń-Wczelik et al. 2014). Researchers concluded that high heat was caused by active CaO and anhydrite which were present in the ashes (Nocuń-Wczelik et al. 2014).

The second heat peak can be associated with the formation of calcium silicate hydrate (CSH) and portlandite (CH) (Taylor 1997). At a 10% replacement rate heat peak, of MS was similar to the control sample; however, in the MFA, the heat peak was significantly higher. Similar

increase in the main peak was also reported in the study of Ataie and Riding (Ataie and Riding 2016), in which 10% of the cement was replaced by high Si fly ash which had originated from the burning of wheat and rice straws. In samples MS 20% and MFA 20%, heat peaks were lower than in the control sample but still higher than in the sample that contained 20% UMS. This could suggest that both replacement materials promote the hydration of tricalcium silicate when 10 or 20% of the cement is replaced. A study conducted by Roszczynialski and Nocuń-Wczelik (Roszczynialski and Nocuń-Wczelik 2004) could provide an alternative explanation. In their study, it was observed that low SO_3 content in relation to calcium aluminate content can cause a significant heat peak which appears after approximately 13 h of curing and is caused by the formation of calcium aluminate hydrates (Roszczynialski and Nocuń-Wczelik 2004). Kaminskas and Cesnauskas (Kaminskas and Cesnauskas 2014) reported that cement replacement by milled biomass fly ash accelerated the hydration of calcium silicates, although the heat of hydration decreased when cement was replaced by milled biomass fly ash.

4.3. Consistency of fresh mortar

Spread values from the flow table test are presented in Fig. 5. Cement replacement by MFA clearly decreased the spread values of the fresh mortar mixtures. However, the difference between the control samples was relatively low at replacement levels of 10 and 20%; hence, super plasticizer was not added to these mixtures. At a 40% replacement level, the flow of fresh mortar was so low that super plasticizer was added to the mixture. After the addition of super plasticizer, the mortar’s consistency returned to the level of the control sample. The dosage of super plasticizer was 0.2% of the binder’s mass which was considered low; the manufacturer of the super plasticizer recommends a dosage of 0.4–2.0%.

Increased water demand related to the utilization of biomass fly ash (Berra et al. 2015; Cuenca et al. 2013; Kaminskas et al. 2015; Rajamma et al. 2009, 2015; Wang et al. 2008) and fluidized

bed combustion fly ash (Li et al. 2012; Rajamma et al. 2015) has been reported in several studies. Gallias et al. (Gallias et al. 2000) reported that increasing the specific surface area of mineral particles correlates with increased water demand in the case of rounded and angular particles. With irregularly shaped particles, a similar correlation was not observed. Water demand of irregularly shaped particles was reported as being two to four times higher than that of rounded or sub-angular mineral particles (Gallias et al. 2000). While the high contents of $CaSO_4$, CaO (Chi and Huang 2014; Li et al. 2012) and unburned organic matter (Chi and Huang 2014; Rajamma et al. 2015) in fluidized bed combustion fly ash have also been reported to cause higher water demand, those were not observed in the fly ash used in this study. Possible reasons for the increased water demand of MFA in this study were likely the combined effects of high specific surface area and irregular particle morphology. However, a small addition of super plasticizer agent returned the spread value of MFA 40% to the control sample's level. This was unlike what was found in a study by Rajamma et al. (Rajamma et al. 2015) in which, even though the mortars also contained super plasticizer agent, the water content had to be increased to obtain proper workability. Because cement replacement with MFA did not decrease the water demand of mortar, we can assume that the filler effect did not significantly impact these samples.

Milling of fly ash clearly had a positive effect on water demand because the spread values of un-milled fly ash in preliminary studies were considerably lower than with MFA (data not shown). It is possible that milling lowered the water demand of the fly ash by lowering the amount of irregularly shaped ash particles (Fu et al. 2008). Similar results related to the positive effects of milling were reported in other studies (Li et al. 2012; Ohenoja et al. 2016a). Notably, the milling does not necessarily cause a significant increase in the specific surface area which can already be quite high for un-milled ash (Ohenoja et al. 2016a). Thus, milling could be an

interesting method for modifying fly ash particle size distribution toward better packing without increasing the specific surface area.

Cement replacement by MS (see Fig. 5) had no clear effect on the spread values of the mortar mixtures. This was expected because the particle size distribution of MS was close to that of cement. Studies have shown that cement replacement with inert mineral particles containing the same particle size distribution does not alter the packing of cement (Gallias et al. 2000; Tikkanen 2013). In this study, the specific surface area of MS and likely also the morphology were similar to those of cement. When the particle size distributions of both materials were close to each other, the water demand was not affected by the replacement of cement with MS. Thus, it can be concluded that MS did not affect the mortar samples' properties via the filler effect.

4.4. XRD analysis of cured paste samples

XRD analysis of hardened cement pastes revealed that replacing a portion of the cement with either MS or MFA did not radically affect the identified hydration products after 7 or 28 d (Figs. 6 and 7). XRD cannot, however, detect possible changes in amorphous hydration products. The crystalline phases identified from the control samples were portlandite, larnite, brownmillerite, calcium carbonate, and monocarboaluminate (Ca_4Al_2 $(CO_3)(OH)_{12}\cdot 5H_2O$). Portlandite is a common hydration product of cement. Brownmillerite and larnite belong to the main phases of cement clinker; therefore, the presence of these phases indicate that a portion of the cement did not react during the first 28 d. Calcium carbonate likely originated from the limestone present in the cement used in this study. Monocarboaluminate has been observed in other studies (Schöler et al. 2015; De Weerdt et al. 2011) when cement was partially replaced by limestone and supplementary cementitious materials.

When a portion of the cement was replaced by MS or MFA the changes in the XRD graphs (Fig. 6) were primarily related to the unreactive crystalline phases of quartz, albite, and microcline which were present in the replacement materials. Even high replacement levels did not dramatically affect the formation of identified hydration products at curing times of 7 or 28 d. The XRD graphs of 7 and 28 d MFA 40% samples were almost identical (Fig. 7), which indicated that the hydration products formed after 7 d of curing were essentially the same as those present at 28 d. This was also the case with the control sample and samples with MS (data not shown). It should be noted that estimations about the amount of formed hydration products based only on XRD graphs should be avoided. For example Fig. 6 shows that, if phases originating from MS are ignored, there are no significant differences at XRD graphs of control sample and MS 40%, while it is obvious that amount of hydration products must be lower for MS 40% sample.

4.5. Mechanical strength of hardened samples

Compressive strengths of mortar samples at different curing times are presented in Fig. 8. Fig. 8a presents compressive strength with a 10% replacement rate, Fig. 8b with 20%, and Fig. 8c with 40%. The compressive strength of MFA 10% was approximately the same as the strength of the control sample (Fig. 8a). The only exception was the 2 d strength which was slightly lower than the strength of the control sample. The strength of MS 10% (Fig. 8a) was lower than in the control sample during the entire time range.

When 20% of the cement was replaced, MFA produced a higher compressive strength than MS (Fig. 8b); however, both compressive strengths were lower than the control sample during the entire period of the study. MS 20% had almost the same early age compressive strength as MFA 20%; however, after 28 and 90 d, it was significantly lower.

When 40% of the cement was replaced, the sample was significantly weaker than the control sample at 2 and 7 d; however, after 28 and 90 d, it performed much better, and the difference between it and the control sample was much lower (Fig. 8c). The compressive strength of MS 40% was at the same level as MFA 40% after 2 d of curing but at longer curing times the compressive strength of MS 40% was substantially lower. At longer curing times, the decrease was closely proportional to the replacement rate. According to Lawrence et al. possible effects of cement replacement by inert mineral materials are dilution, filler, and nucleation effects and with pozzolanic materials, also the pozzolanic effect (Lawrence et al. 2005).

When the compressive strengths of samples with replacement materials were compared with the control sample, the relative strengths were lower after 2 d of curing than with longer curing times. Thus, replacing cement with MS or MFA more negatively impacted early strength. Importantly, the differences between MFA and MS were quite low after 2 d of hardening, which suggested that the chemical properties of the replacement materials were non-relevant in the early ages. Similar observations were also reported in a study by Lawrence et al. (Lawrence et al. 2005) who also concluded that the surface areas of cement replacement materials correlated with nucleation and the pozzolanic effect. However, regarding inert material increasing fineness above 500 m^2/kg (Blaine) did not give additional strength via the nucleation effect (Lawrence et al. 2005). With pozzolanic material, a similar limit was not observed; hence, increasing fineness above 500 m^2/kg (Blaine) produced higher strength. Researchers also discovered that although the positive effect of heterogeneous nucleation has greater significance in the early ages it is still maintained at longer curing times (Lawrence et al. 2005). It is hard to accurately estimate the role of heterogeneous nucleation in the experiments of this study because only two different replacement materials with different specific surface areas were used. In both cases, at 10 and 20% replacement levels, more heat was generated than with UMS, which could be due to the nucleation effect. However, the compressive strengths in these samples were lower

than the control sample; thus, the high heat of hydration did not result in high compressive strengths. MS and MFA both possessed a high specific surface area which has been reported to promote the nucleation effect (Lawrence et al. 2003; Tikkanen 2013); however, from basis of data from the present study it is impossible evaluate how the high specific surface area affected the compressive strengths of the mortars. The compressive strengths of the samples containing MFA increased between 2 and 28 d more than mortars with MS, which indicated that good of mechanical strength not induced by nucleation effects only. According to Cyr et al. (2006), strength gain due to pozzolanic properties overtake the nucleation effect after 28 d. However, certain studies (Berra et al. 2015; Kaminskas and Cesnauskas 2014) have suggested that some biomass fly ashes do not possess significant pozzolanic properties. In this study, no significant strength increase was observed after 28 d, which indicated that the pozzolanic effect was not dominant in this case.

Several studies (Dung et al. 2014, 2015a; b; Salain et al. 2001; Wu et al. 2015) have demonstrated that fly ash from fluidized bed combustion can activate the latent hydraulic properties of blast furnace slag which was also one constituent of the cement used in this study. Notably, this effect was considered to be low or insignificant because contents of CaO (Dung et al. 2015b), free CaO (Salain et al. 2001), and SO_3 (Wu et al. 2015; Salain et al. 2001), which are associated with the activation of blast furnace slag, were relatively low in the fly ash used in this study compared to ashes used in other studies. The CaO and SO_3 contents of MFA were even lower than in the cement used in this study; therefore, it is unlikely that replacing cement with MFA could further promote the hydration of blast furnace slag.

It is known that fly ashes from fluidized bed combustion can possess moderate hydraulic properties (Li et al. 2012; Nocuń-Wczelik et al. 2014; Ohenoja et al. 2016a; Zhao et al. 2015). Ohenoja et al. observed that self-hardening samples produced from milled fly ash from fluidized bed combustion of peat and forest industry residuals can reach up to a 20 MPa hydraulic

compressive strength (Ohenoja et al. 2016a). Similar compressive strengths have also been measured in self-hardening samples prepared from fly ash from the fluidized bed combustion of coal (Li et al. 2012). Results from the selective dissolution method also indicated that the fly ash used in this study contained components that can take part to hydration reactions. Thus increase in compressive strength, related to cement replacement by MFA, could originate from slow hydration of the Ca, Si, Al, and S bearing phases (Illikainen et al. 2014; Ohenoja et al. 2016a). The formed hydration products were essentially the same as those formed in the hydration of plain cement because no distinctive hydration products were observed in the XRD analysis. Portions of the selectively soluble components were estimated to be sufficient to form a significant amount of hydration products which could compensate for the adverse dilution effect caused by cement replacement.

The flexural strengths of the mortar samples at different curing times are presented at Fig. 9. Fig. 9a presents flexural strength with a 10% replacement rate, Fig. 9b with 20%, and Fig. 9c with 40%. When 10% of the cement was replaced by either MFA or MS, the flexural strengths of the samples were at the same level as the strength of the control sample (Fig. 9a). Decline in the flexural strength of control sample and MFA 10% was observed after 28 d. This phenomena is probably related to variation of measurements, especially at the case of control sample which had the greatest error, since no other reasonable explanation was found. When 20% of the cement was replaced, the flexural strengths behaved in a similar way to the 10% replacement; however, in the early age, the strengths were slightly lower (Fig. 9b). At a 40% replacement with MS, the decrease in flexural strength was significant; however, MFA produced similar flexural strength than the control sample after 90 d of curing, even with a 40% replacement level (Fig. 9c); however, shorter curing time decreased the strength significantly compared to the control sample.

5 Conclusions

Fly ash from fluidized bed combustion of peat and forest industry residuals offer a potential alternative cement replacement material. With low cement replacement ratios (10 and 20%), it is possible to achieve almost the same compressive strength—more than 90%—as that of the control sample. By replacing 40% of cement by fly ash, the compressive strength can be still as high as 88% of the control sample's strength. Compared to un-reactive material, the difference at the early stage of hydration is low; therefore, the nucleation effect of fly ash is not dominant. The studied fly ash possesses hydraulic properties, which explains positive effects on strength. While this work revealed that fluidized bed combustion ash show potential as a cement replacement material, further studies are needed, especially given the large variation in the current fluidized bed combustion fly ashes.

Acknowledgements

This work was done under the auspices of the "MINSI" project, which is supported by The European Regional Development Fund (ERDF), and various companies including Ekokem, Pohjolan Voima, Oulun Energia, SSAB, and Stora Enso. We would like to thank Mr. Sami Saukko (Center of Microscopy and Nanotechnology, University of Oulu) and Mr. Pekka Tanskanen (Process Metallurgy, University of Oulu) for their help and guidance related to the x-ray diffraction analysis. Mr. Jarno Karvonen and Mr. Jani Österlund are acknowledged for their contributions to the laboratory work.

References

Abdul Awal, A. S. M. (2013). "Influence of high volume fly ash in controlling heat of hydration of concrete." *International Journal of Engineering Research and Applications (IJERA)*, 2(3), 932–938.

Ataie, F. F., and Riding, K. A. (2016). "Influence of agricultural residue ash on early cement hydration and chemical admixtures adsorption." *Construction and Building Materials*, 106, 274–281.

Berra, M., Mangialardi, T., and Paolini, A. E. (2015). "Reuse of woody biomass fly ash in cement-based materials." *Construction and Building Materials*, 76, 286–296.

Chi, M., and Huang, R. (2014). "Effect of circulating fluidized bed combustion ash on the properties of roller compacted concrete." *Cement and Concrete Composites*, 45, 148–156.

Chindaprasirt, P., Rattanasak, U., and Jaturapitakkul, C. (2011). "Utilization of fly ash blends from pulverized coal and fluidized bed combustions in geopolymeric materials." *Cement and Concrete Composites*, 33(1), 55–60.

Cuenca, J., Rodríguez, J., Martín-Morales, M., Sánchez-Roldán, Z., and Zamorano, M. (2013). "Effects of olive residue biomass fly ash as filler in self-compacting concrete." *Construction and Building Materials*, Special Section on Recycling Wastes for Use as Construction Materials, 40, 702–709.

Cyr, M., Lawrence, P., and Ringot, E. (2006). "Efficiency of mineral admixtures in mortars: Quantification of the physical and chemical effects of fine admixtures in relation with compressive strength." *Cement and Concrete Research*, 36(2), 264–277.

Dung, N. T., Chang, T.-P., and Chen, C.-T. (2015a). "Hydration process and compressive strength of slag-CFBC fly ash materials without portland cement." *Journal of Materials in Civil Engineering*, 27(7).

Dung, N. T., Chang, T.-P., Chen, C.-T., and Yang, T.-R. (2015b). "Cementitious properties and microstructure of an innovative slag eco-binder." *Materials and Structures*, 1–16.

Dung, N. T., Chang, T.-P., and Yang, T.-R. (2014). "Performance evaluation of an eco-binder made with slag and CFBC fly ash." *Journal of Materials in Civil Engineering*, 26(12).

Dyson, H. M., Richardson, I. G., and Brough, A. R. (2007). "A Combined 29Si MAS NMR and Selective Dissolution Technique for the Quantitative Evaluation of Hydrated Blast Furnace Slag Cement Blends." *Journal of the American Ceramic Society*, 90(2), 598–602.

Van Eijk, R. J., Obernberger, I., and Supancic, K. (2012). *Options for increased utilization of ash from biomass combustion and co-firing*. IEA Bioenergy Task 32, Arnhem.

Fu, X., Li, Q., Zhai, J., Sheng, G., and Li, F. (2008). "The physical–chemical characterization of mechanically-treated CFBC fly ash." *Cement and Concrete Composites*, 30(3), 220–226.

Gallias, J. L., Kara-Ali, R., and Bigas, J. P. (2000). "The effect of fine mineral admixtures on water requirement of cement pastes." *Cement and Concrete Research*, 30(10), 1543–1549.

Haha, M. B., De Weerdt, K., and Lothenbach, B. (2010). "Quantification of the degree of reaction of fly ash." *Cement and Concrete Research*, 40(11), 1620–1629.

Han, F., Liu, R., Wang, D., and Yan, P. (2014). "Characteristics of the hydration heat evolution of composite binder at different hydrating temperature." *Thermochimica Acta*, 586, 52–57.

Illikainen, M., Tanskanen, P., Kinnunen, P., Körkkö, M., Peltosaari, O., Wigren, V., Österbacka, J., Talling, B., and Niinimäki, J. (2014). "Reactivity and self-hardening of fly ash from the fluidized bed combustion of wood and peat." *Fuel*, 135, 69–75.

Kaminskas, R., and Cesnauskas, V. (2014). "Influence of activated biomass fly ash on portland cement hydration." *Ceramics - Silikaty*, 58(4), 260–268.

Kaminskas, R., Cesnauskas, V., and Kubiliute, R. (2015). "Influence of different artificial additives on Portland cement hydration and hardening." *Construction and Building Materials*, 95, 537–544.

Korpijärvi, K., Mroueh, U.-M., Merta, E., Laine-Ylijoki, J., Harri, K., Järvelä, E., Wahlström, M., and Mäkelä, E. (2009). *Energiantuotannon tuhkien jalostaminen maarakennuskäyttöön.* VTT, Espoo.

Lawrence, P., Cyr, M., and Ringot, E. (2003). "Mineral admixtures in mortars: Effect of inert materials on short-term hydration." *Cement and Concrete Research*, 33(12), 1939–1947.

Lawrence, P., Cyr, M., and Ringot, E. (2005). "Mineral admixtures in mortars effect of type, amount and fineness of fine constituents on compressive strength." *Cement and Concrete Research*, 35(6), 1092–1105.

Li, X., Chen, Q., Huang, K., Ma, B., and Wu, B. (2012). "Cementitious properties and hydration mechanism of circulating fluidized bed combustion (CFBC) desulfurization ashes." *Construction and Building Materials*, 36, 182–187.

Loo, S. van, Koppejan, J., and Dawsonera (Eds.). (2008). *The handbook of biomass combustion and co-firing*. Earthscan, London.

Luke, K., and Glasser, F. P. (1987). "Selective dissolution of hydrated blast furnace slag cements." *Cement and Concrete Research*, 17(2), 273–282.

Nocuń-Wczelik, W., Łagosz, A., Kowalski, B., and Gawlicki, M. (2014). "Calorimetry in testing waste materials from the brown coal combustion." *Journal of Thermal Analysis & Calorimetry*, 118(1), 123–131.

Ohenoja, K., Tanskanen, P., Peltosaari, O., Wigren, V., Österbacka, J., and Illikainen, M. (2016a). "Effect of particle size distribution on the self-hardening property of biomass-peat fly ash from a bubbling fluidized bed combustion." *Fuel Processing Technology*, 148, 60–66.

Ohenoja, K., Tanskanen, P., Wigren, V., Kinnunen, P., Körkkö, M., Peltosaari, O., Österbacka, J., and Illikainen, M. (2016b). "Self-hardening of fly ashes from a bubbling fluidized bed combustion of peat, forest industry residuals, and wastes." *Fuel*, 165, 440–446.

Pavoine, A., Harbec, D., Chaussadent, T., Tagnit-Hamou, A., and Divet, L. (2014). "Impact of Alternative Cementitious Material on Mechanical and Transfer Properties of Concrete." *Materials Journal*, 111(3), 251–262.

Rajamma, R., Ball, R. J., Tarelho, L. A. C., Allen, G. C., Labrincha, J. A., and Ferreira, V. M. (2009). "Characterisation and use of biomass fly ash in cement-based materials." *Journal of Hazardous Materials*, 172(2–3), 1049–1060.

Rajamma, R., Senff, L., Ribeiro, M. J., Labrincha, J. A., Ball, R. J., Allen, G. C., and Ferreira, V. M. (2015). "Biomass fly ash effect on fresh and hardened state properties of cement based materials." *Composites Part B: Engineering*, 77, 1–9.

Roszczynialski, W., and Nocuń-Wczelik, W. (2004). "Studies of cementitious systems with new generation by-products from fluidised bed combustion." *Journal of Thermal Analysis and Calorimetry*, 77(1), 151–158.

Salain, I. M. a. K., Clastres, P., Bursi, J. M., and Pellissier, and C. (2001). "Circulating Fluidized Bed Combustion Ashes as an Activator of Ground Vitrified Blast Furnace Slag." *Special Publication*, 202, 225–244.

Sata, V., Tangpagasit, J., Jaturapitakkul, C., and Chindaprasirt, P. (2012). "Effect of W/B ratios on pozzolanic reaction of biomass ashes in Portland cement matrix." *Cement and Concrete Composites*, 34(1), 94–100.

Schöler, A., Lothenbach, B., Winnefeld, F., and Zajac, M. (2015). "Hydration of quaternary Portland cement blends containing blast-furnace slag, siliceous fly ash and limestone powder." *Cement and Concrete Composites*, 55, 374–382.

524 SFS (Finnish Standards Association). (1999). *"Methods of test for mortar for masonry. Part 3:*
525 *Determination of consistence of fresh mortar (by flow table)" SFS-EN 1015-3:en.*
526 SFS (Finnish Standards Association). (2013). *"Fly ash for concrete. Part 1: Definition,*
527 *specifications and conformity criteria" SFS·EN 450-1:en.*
528 SFS (Finnish Standards Association). (2016). *"Methods of testing cement. Part 1:*
529 *Determination of strength" SFS-EN 196-1:2016:en.*
530 Sinsiri, T., Chindaprasirt, P., and Jaturapitakkul, C. (2010). "Influence of fly ash fineness and
531 shape on the porosity and permeability of blended cement pastes." *International Journal*
532 *of Minerals, Metallurgy, and Materials*, 17(6), 683–690.
533 Taylor, H. F. W. (1997). *Cement Chemistry*. Thomas Telford, London.
534 Teixeira, E. R., Mateus, R., Camões, A. F., Bragança, L., and Branco, F. G. (2016).
535 "Comparative environmental life-cycle analysis of concretes using biomass and coal fly
536 ashes as partial cement replacement material." *Journal of Cleaner Production*, 112, Part
537 4, 2221–2230.
538 Tikkanen, J. (2013). *A novel application of mineral powders in normal strength concrete*
539 (Doctoral dissertation). Aalto University, Helsinki.
540 Wang, S., Miller, A., Llamazos, E., Fonseca, F., and Baxter, L. (2008). "Biomass fly ash in
541 concrete: Mixture proportioning and mechanical properties." *Fuel*, 87(3), 365–371.
542 De Weerdt, K., Kjellsen, K. O., Sellevold, E., and Justnes, H. (2011). "Synergy between fly ash
543 and limestone powder in ternary cements." *Cement and Concrete Composites*, 33(1),
544 30–38.
545 Wu, T., Chi, M., and Huang, R. (2014). "Characteristics of CFBC fly ash and properties of
546 cement-based composites with CFBC fly ash and coal-fired fly ash." *Construction and*
547 *Building Materials*, 66, 172–180.

548 Wu, Y.-H., Huang, R., Tsai, C.-J., and Lin, W.-T. (2015). "Utilizing residues of CFB co-
549 combustion of coal, sludge and TDF as an alkali activator in eco-binder." *Construction*
550 *and Building Materials*, 80, 69–75.
551 Zhao, J., Wang, D., and Liao, S. (2015). "Effect of mechanical grinding on physical and
552 chemical characteristics of circulating fluidized bed fly ash from coal gangue power
553 plant." *Construction and Building Materials*, 101, Part 1, 851–860.
554

Table 1. Design of mortar mixtures

mixture	cement [g]	milled ash [g]	milled sand [g]	CEN standard sand [g]	water [g]	super plasticizer [ml]
control	450 ± 1	0	0	1350 ± 3	225 ± 1	0
MS 10%	405 ± 1	0	45 ± 1	1350 ± 3	225 ± 1	0
MS 20%	360 ± 1	0	90 ± 1	1350 ± 3	225 ± 1	0
MS 40%	270 ± 1	0	180 ± 1	1350 ± 3	225 ± 1	0
MFA 10%	405 ± 1	45 ± 1	0	1350 ± 3	225 ± 1	0
MFA 20%	360 ± 1	90 ± 1	0	1350 ± 3	225 ± 1	0
MFA 40%	270 ± 1	180 ± 1	0	1350 ± 3	225 ± 1	1

Table 2. Chemical composition of cement, MS, and MFA

Sample name	cement	MS	MFA
CaO, XRF (%)	58.4	1.6	16.3
SiO_2, XRF (%)	21.7	77.0	41.8
Al_2O_3, XRF (%)	5.4	12.1	13.1
Fe_2O_3, XRF (%)	3.3	2.1	13.6
Na_2O, XRF (%)	0.6	3.1	2.1
K_2O, XRF (%)	0.7	3.0	2.3
MgO, XRF (%)	3.9	0.6	2.5
P_2O_5, XRF (%)	0.1	0.1	3.5
TiO_2, XRF (%)	0.6	0.2	0.5
SO_3, XRF (%)	3.5	0.0	2.1
Cl, XRF (%)	0.1	N/A	0.1
Selectively soluble CaO (%)	N/A	N/A	10.6
Selectively soluble SiO_2 (%)	N/A	N/A	1.8
Selectively soluble Al_2O_3 (%)	N/A	N/A	1.5
Selectively soluble Fe_2O_3 (%)	N/A	N/A	0.8
Free CaO (%)	N/A	N/A	2.5
Loss on ignition 950 C° (%)	3.4	0.4	0.3

Figure

Click here to download Figure FIG1.tif

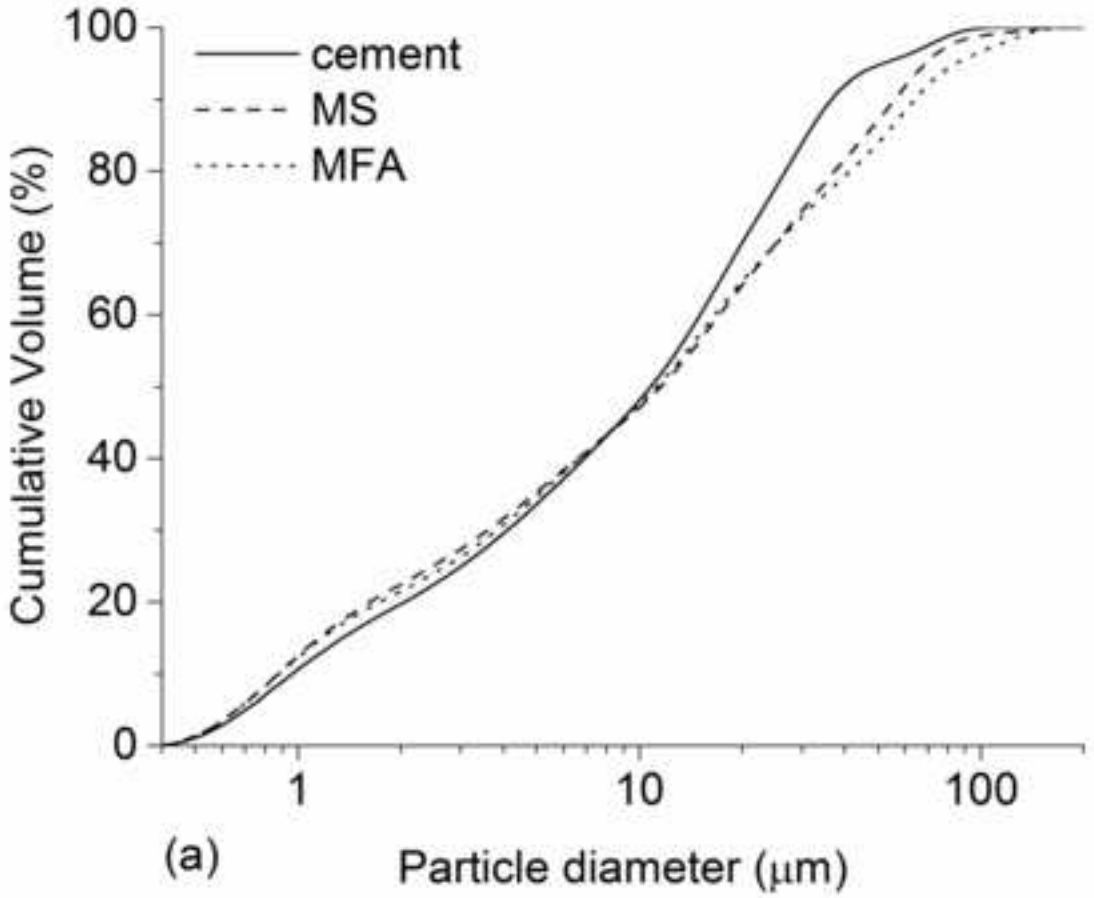

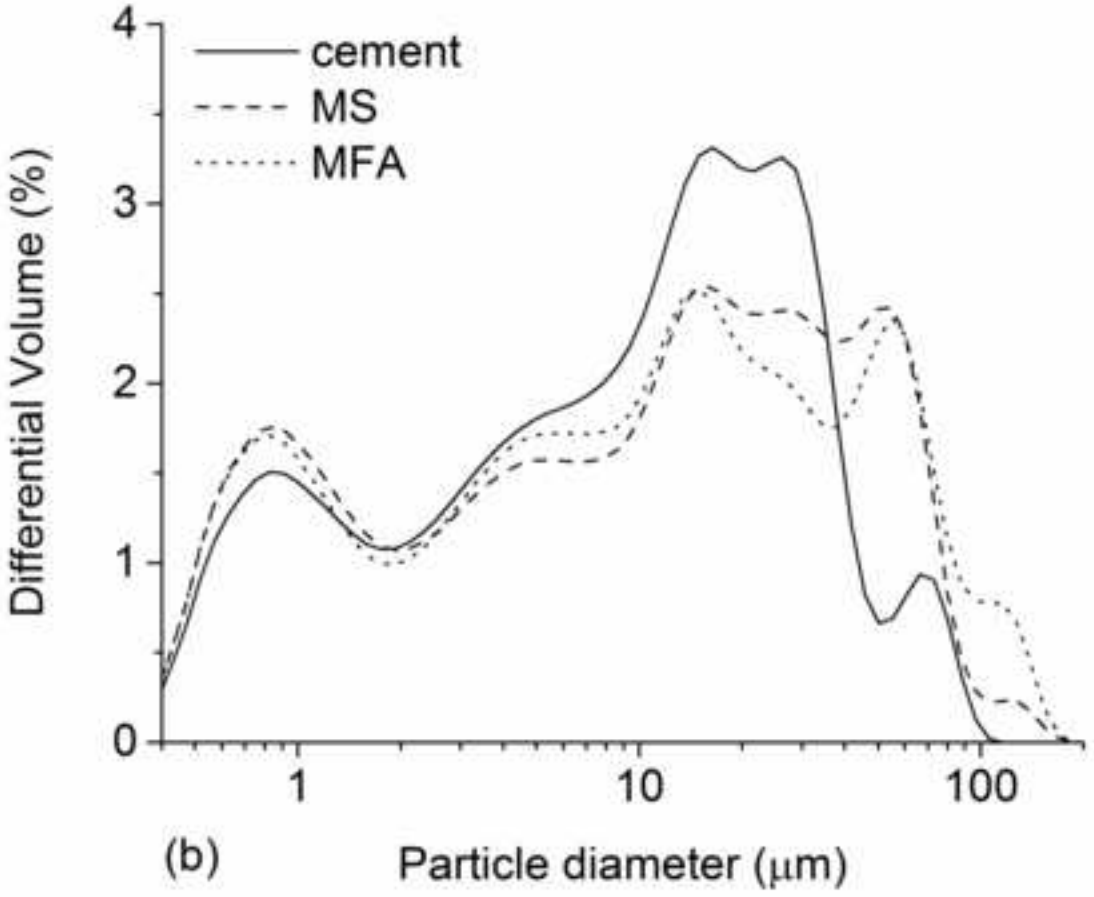

Figure

Click here to download Figure FIG2.tif

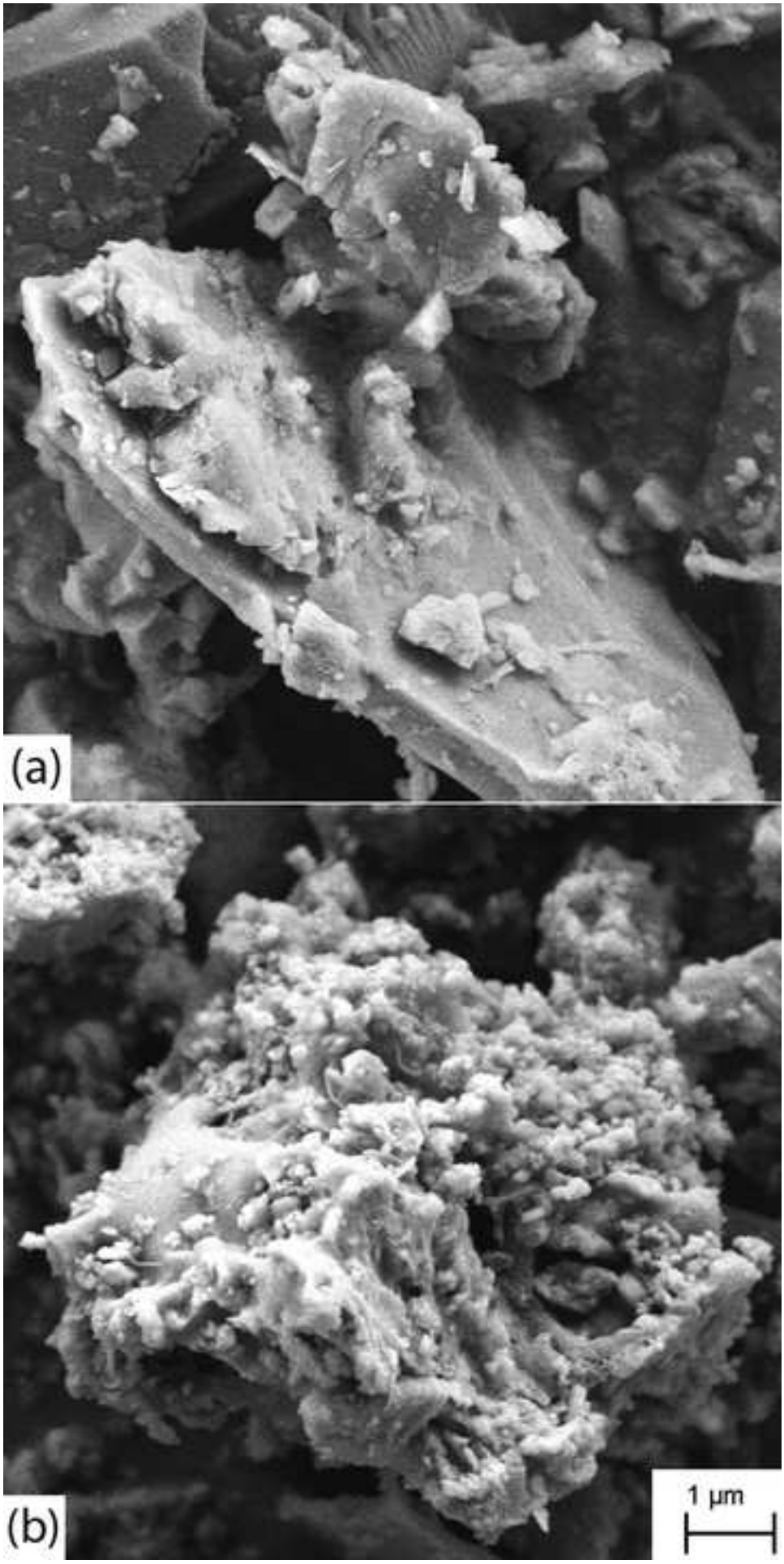

Figure

Click here to download Figure FIG3.tif

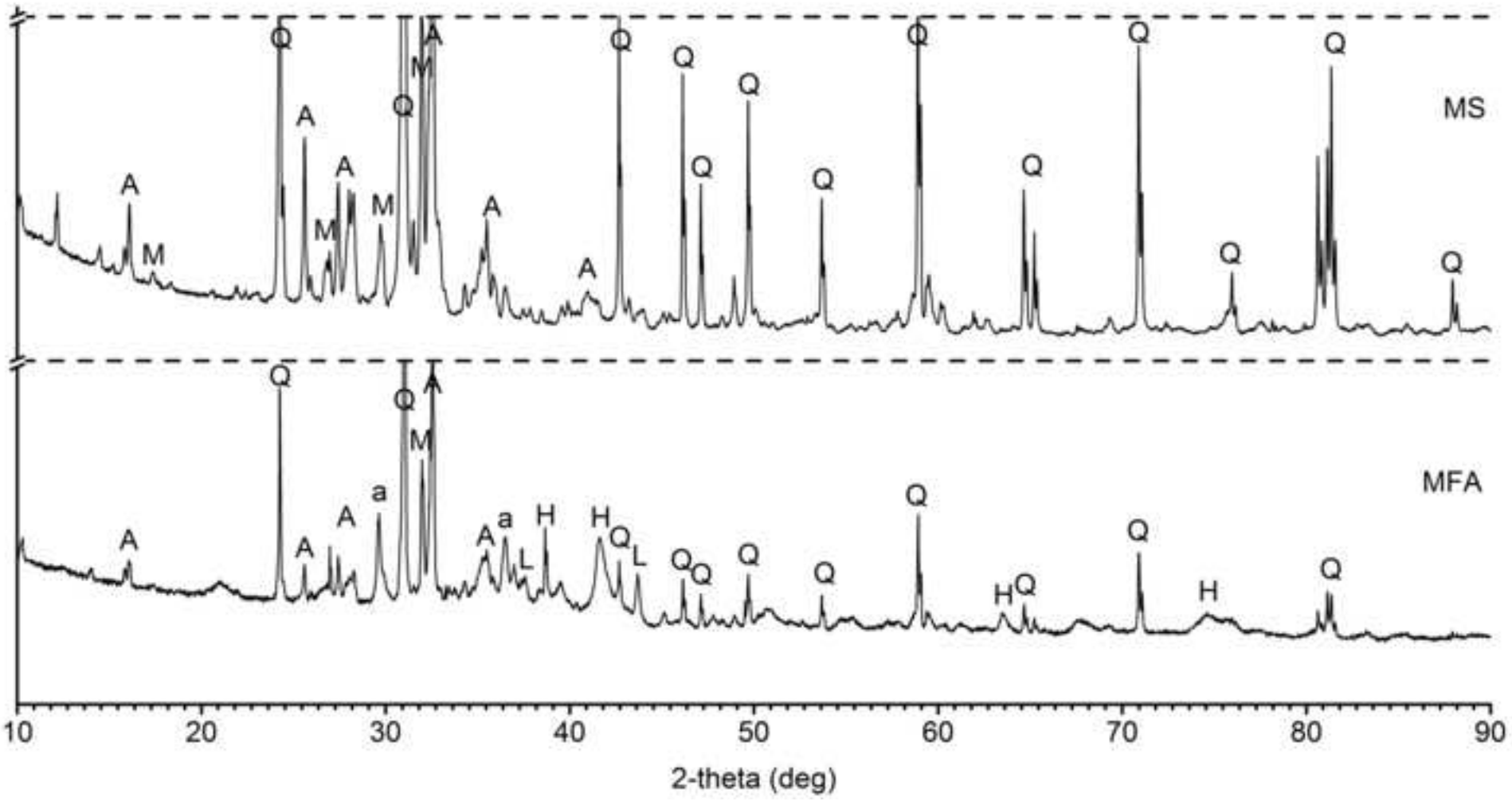

Figure

Click here to download Figure FIG4.tif

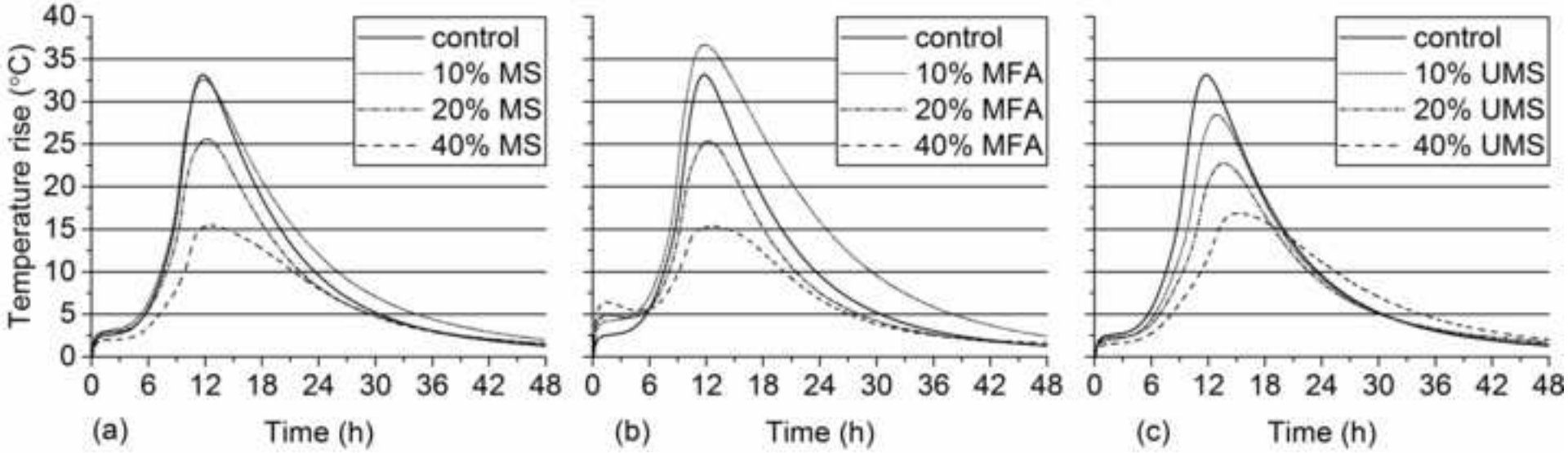

Figure

Click here to download Figure FIG5.tif

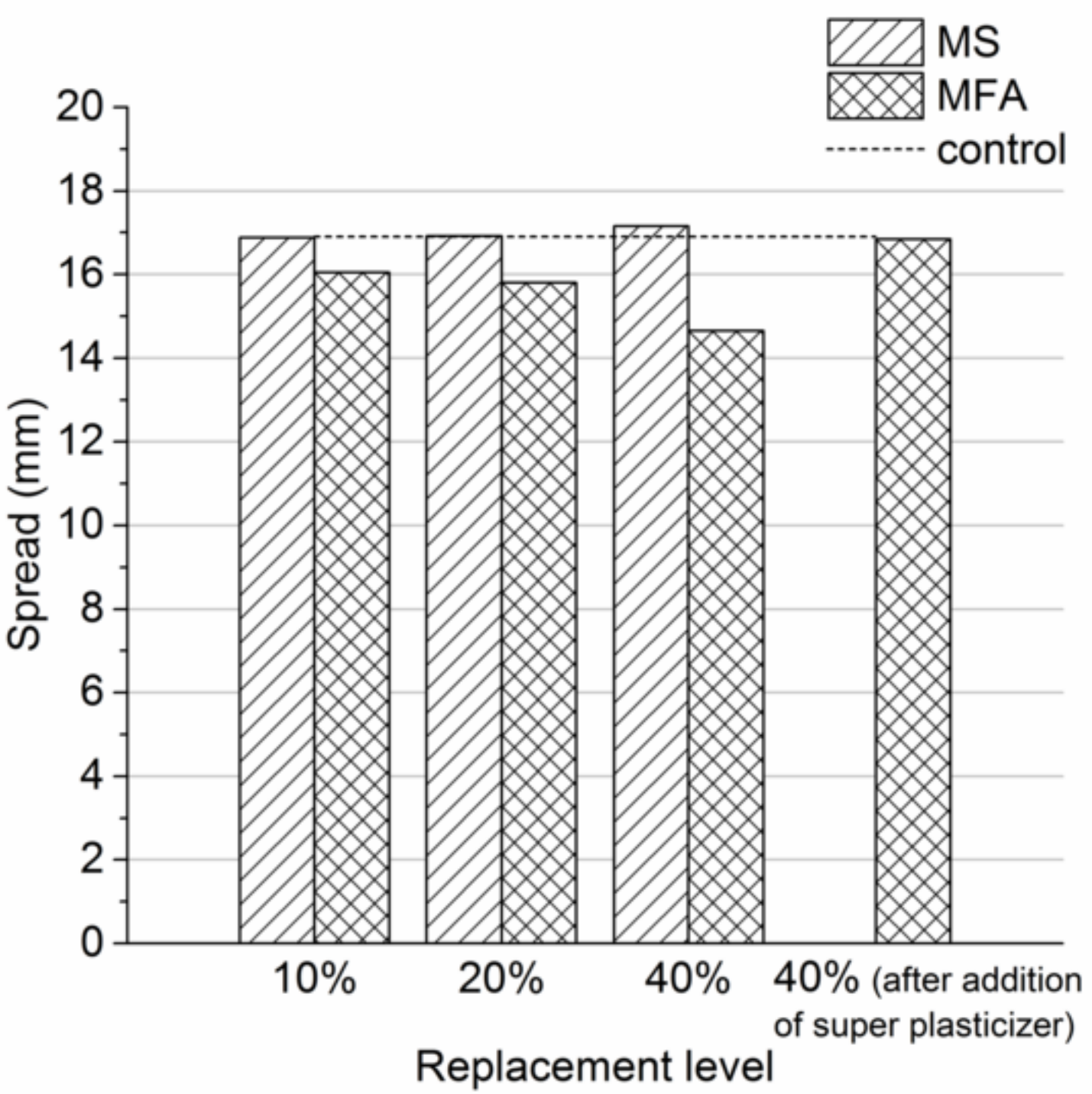

Figure

Click here to download Figure FIG6.tif

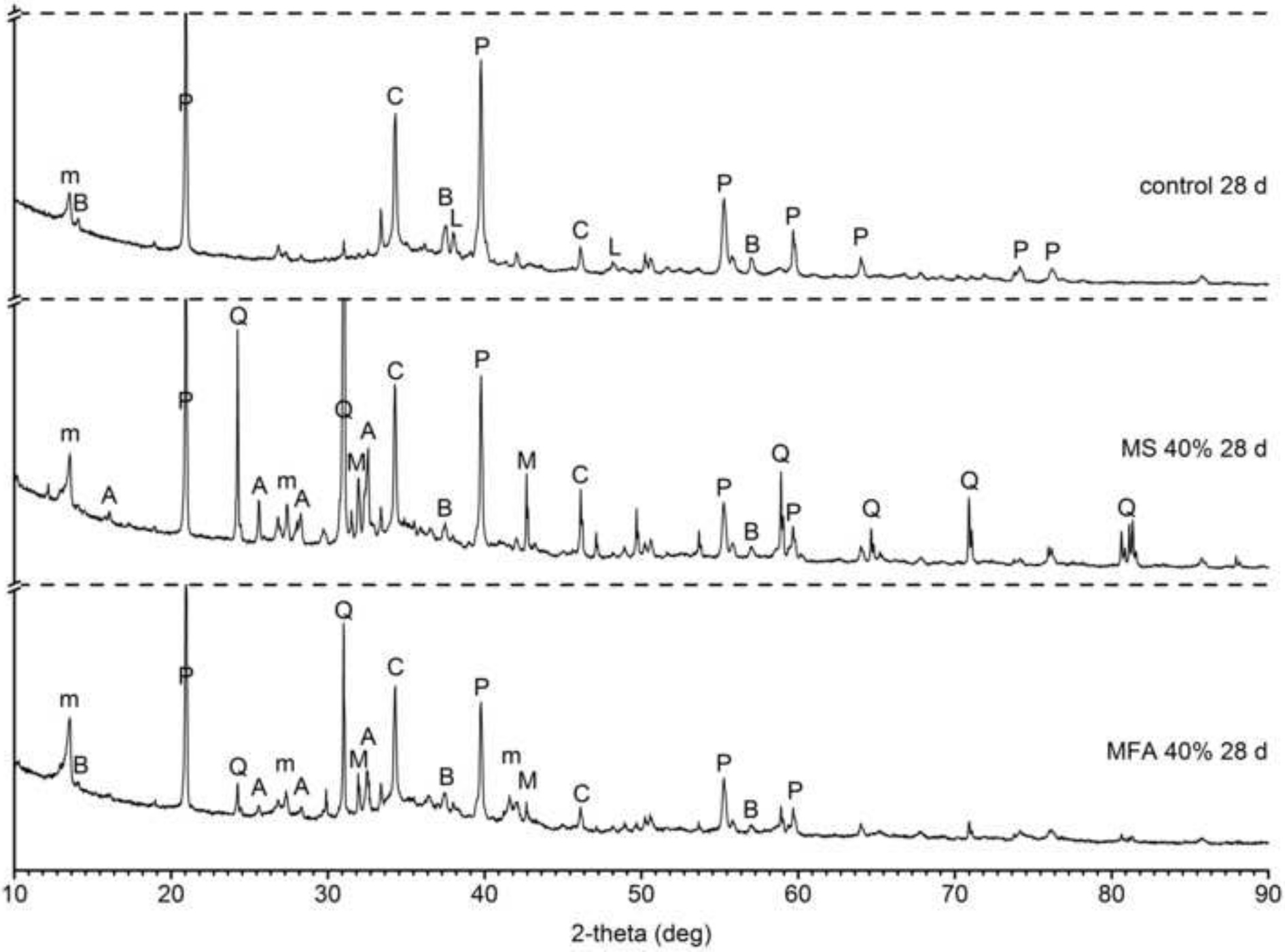

Figure

Click here to download Figure FIG7.tif

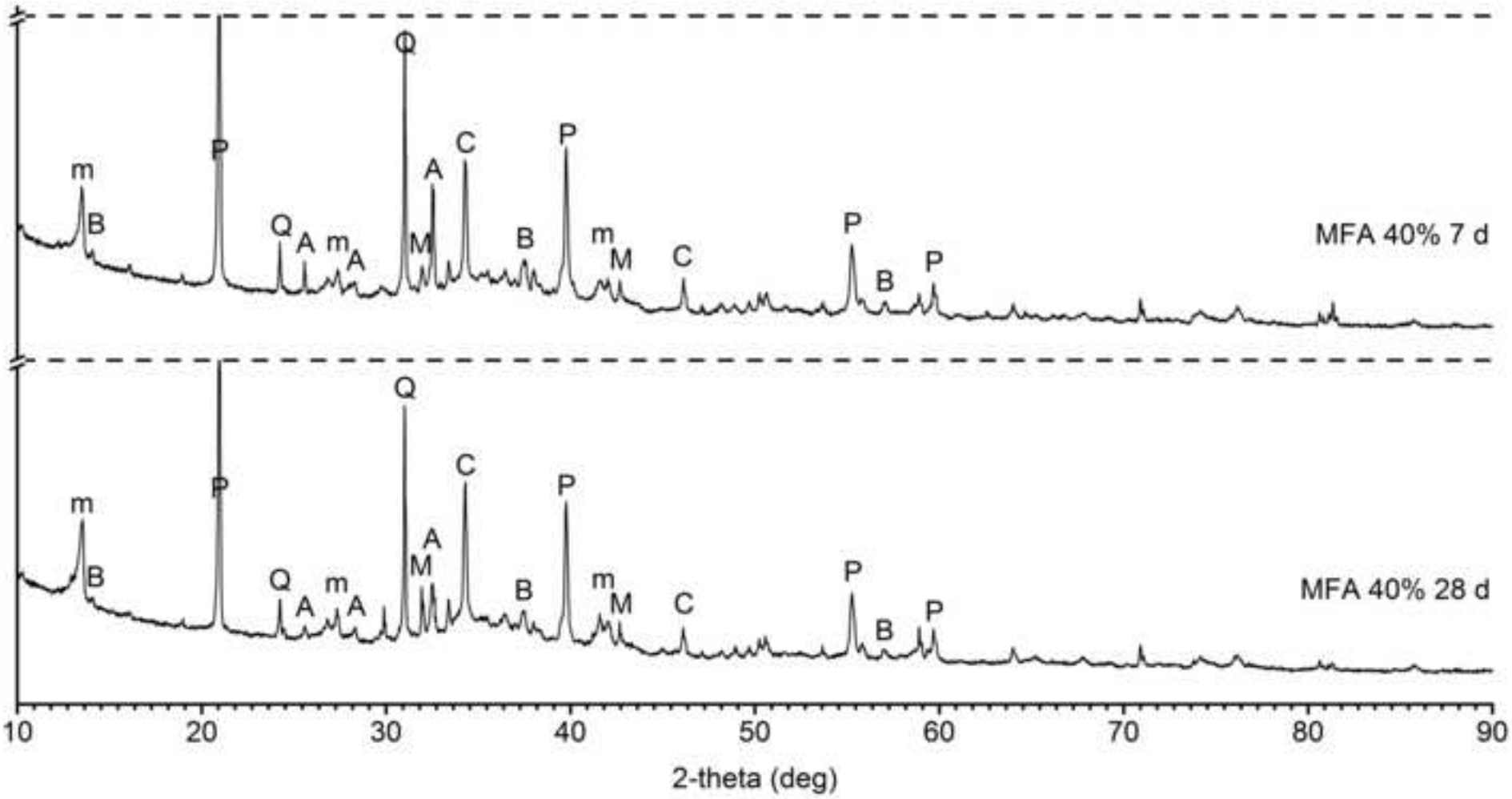

Figure

Click here to download Figure FIG8.tif

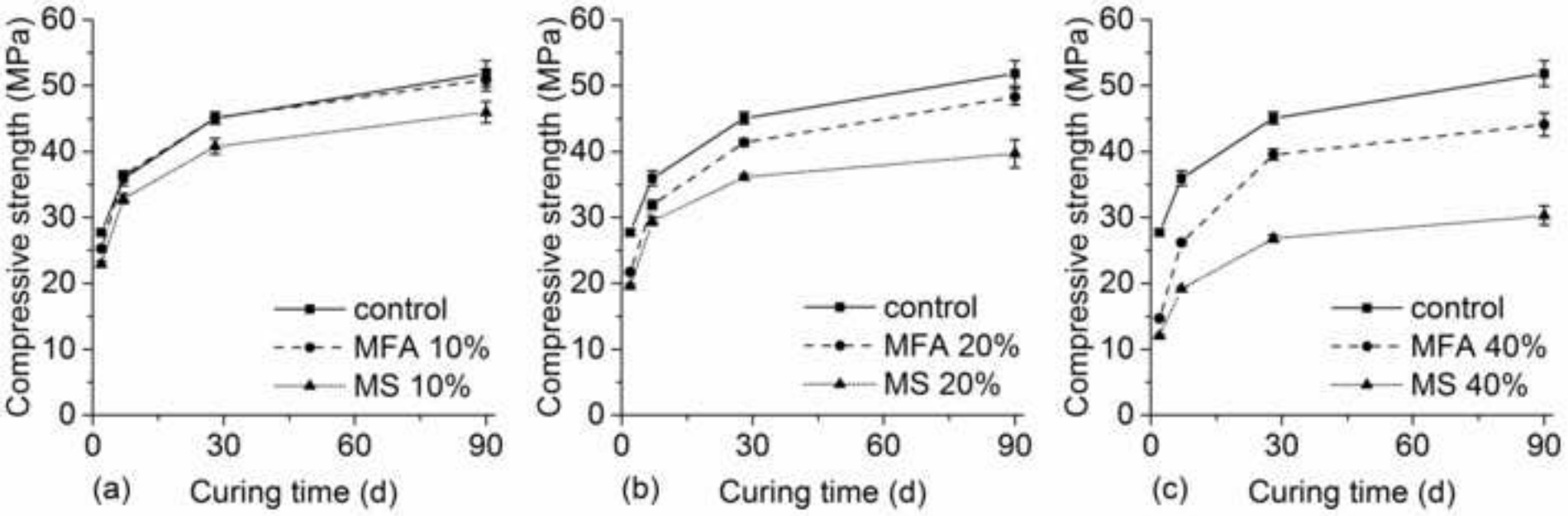

Figure

Click here to download Figure FIG9.tif

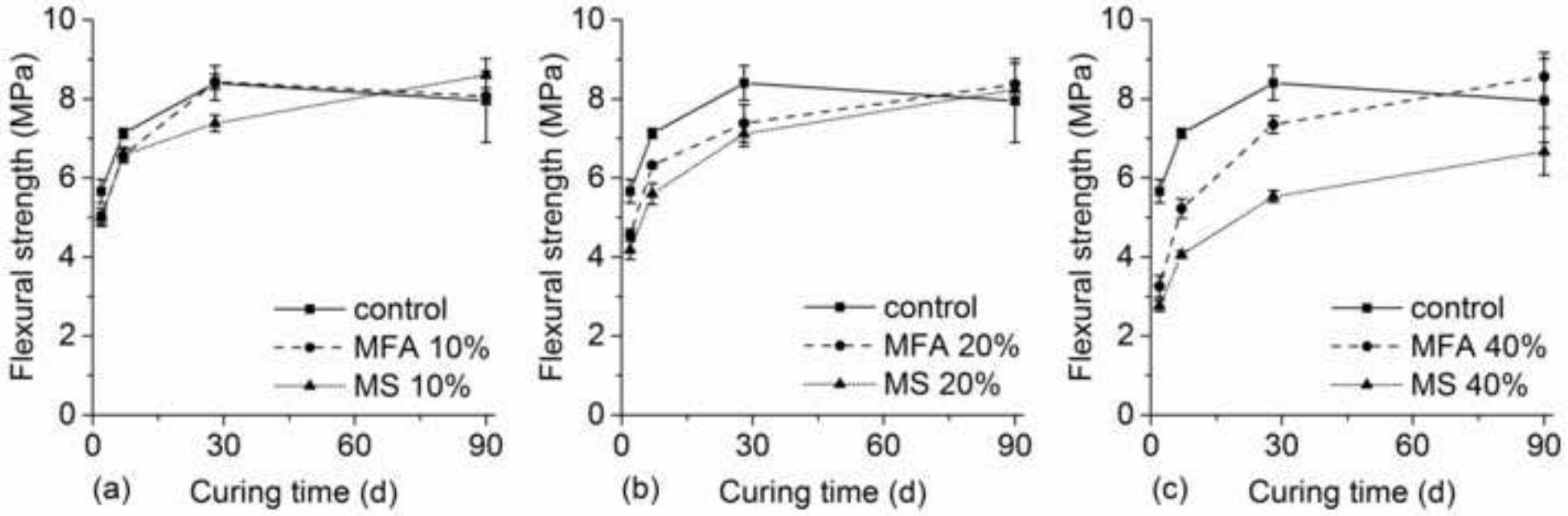

Figure captions

Fig. 1. Particle size distribution of materials, (a) cumulative and (b) differential

Fig. 2. FESEM pictures of MS (a) and MFA (b)

Fig. 3. XRD graphs of MS and MFA: A = albite, a = anhydrite, H = hematite, L = lime, M = microcline, and Q = quartz

Fig. 4. Results of semi-adiabatic calorimetry of (a) MS, (b) MFA, and (c) UMS

Fig. 5. Spread values of mortar samples

Fig. 6. XRD graphs of the control 28 d, MS 40% 28d, and MFA 40% 28 d: A = albite, B = brownmillerite, C = calcite, m = calcium monocarboaluminate, L = larnite, M = microcline, P = portlandite, and Q = quartz

Fig. 7. XRD graphs of MFA 40% 7 d and MFA 40% 28 d: A = albite, B = brownmillerite, C = calcite, m = monocarboaluminate, L = larnite, M = microcline, P = portlandite, and Q = quartz

Fig. 8. Compressive strengths of samples at the (a) 10%, (b) 20%, and (c) 40% replacement levels

Fig. 9. Flexural strengths of samples at the (a) 10%, (b) 20%, and (c) 40% replacement levels